Saudi Pharmaceutical Journal 27 (2019) 1000–1008

Contents lists available at ScienceDirect

Saudi Pharmaceutical Journal

journal homepage: www.sciencedirect.com

Gastric floating sustained-release tablet for dihydromyricetin: Development, characterization, and pharmacokinetics study

Hao Liu [a,*], Wenmei Zhao [a], Qi Hu [a], Ling Zhao [a], Yumeng Wei [a], Chao Pi [a], Yuhan Yang [a], Xuerong Yang [a], Hang Yuan [a], Yuhan Zhang [b], Kunyan Qu [a], Xinyu Shi [a], Yao Huang [a], Houyin Shi [c,*]

[a] School of Pharmacy, Southwest Medical University, Luzhou City, Sichuan, People's Republic of China
[b] School of Clinical Medicine, Southwest Medical University, Luzhou City, Sichuan, People's Republic of China
[c] Department of Orthopedics, The Affiliated Traditional Chinese Medicine Hospital of Southwest Medical University, Luzhou City, Sichuan, People's Republic of China

ARTICLE INFO

Article history:
Received 9 May 2019
Accepted 7 August 2019
Available online 8 August 2019

Keywords:
Gastric floating tablet
Sustained release
Dihydromyricetin
Stability
Pharmacokinetics
Bioavailability

ABSTRACT

Dihydromyricetin (DHM) is a natural dihydroflavonol compound with quite a number of important pharmacological properties. However, its low solubility in water and poor stability in aqueous environment, have compromised drug efficacy of DHM, thus hindering its clinical use. The present study was to develop DHM-loaded gastric floating sustained-release tablet (DHM-GFT) to improve the bioavailability of DHM. DHM-GFT was prepared via powder direct compression. The formulation of tablet was optimized in terms of the floating ability and drug release rate. The optimized DHM-GFT exhibited short floating lag time of less than 10 s and long floating duration of over 12 h in acidic medium. It had a 12-hour sustained release of DHM, which proved its potential to develop as a twice-a-day dosing preparation. The physicochemical properties of DHM-GFT well satisfied the pharmacopoeial requirements. In addition, the results from pharmacokinetic studies demonstrated that, DHM-GFT could considerably prolong the *in vivo* residence time of drug and improve the bioavailability via good gastric floating ability and sustained drug release when compared to DHM powder. Therefore, DHM-GFT is promising to promote the application of DHM and merits studies for further development.

1. Introduction

Dihydromyricetin (DHM), also known as ampelopsin, is a natural dihydroflavonol compound (Fig. 1) widely found in plants such as Vitis, Garcinia, and Myricaceae. Over the past ten years, the pharmacological effects of DHM have been intensively studied. DHM was reported to possess several important pharmacological properties, including but not limited to anti-oxidation, anti-inflammatory, anti-cancer, and antimicrobial activities. These properties showed great potential for pharmaceutical development (Li et al., 2018; Zhang et al., 2018). Currently, commercially available DHM preparations are still rare, and studies on different DHM preparations are ongoing in order to promote the clinical applications of this promising drug. DHM has low water solubility (only about 0.2 mg/ml at 25 °C) and poor stability in aqueous environments. It is also very sensitive to environmental factors such as light, oxygen, and the pH of aqueous solvents. Particularly, the dissolved DHM is relatively stable only under acidic conditions. During our previous investigations, it was found that the hydroxyl groups of DHM molecule can start to dissociate when the pH is raised to 7. When the pH is >10, oxidation and ring-opening reactions of the drug molecule are likely to occur, leading to significant changes in the molecular configuration. The above defects have led to compromised drug efficacy of DHM, which usually requires high doses for treatment (Li et al., 2019; Liu et al., 2017; Xiang et al., 2018).

To enhance the solubility of DHM, methods involving the use of suitable cosolvents, such as ethanol and DMSO, can be employed to facilitate the dissolution of the drug. However, these organic solvents can be problematic for application. Another possible method involves using suitable drug carriers to facilitate the dissolution of

* Corresponding authors at: Department of Pharmaceutics, School of Pharmacy, Southwest Medical University, No. 319 Section 3, Zhongshan Road, Luzhou City, Sichuan Province 646000, People's Republic of China (H. Liu). Department of Orthopedics, The Affiliated Traditional Chinese Medicine Hospital of Southwest Medical University, No. 182 Chunhui Road, Longmatan District, Luzhou City, Sichuan Province 646000, People's Republic of China (H. Shi).
E-mail addresses: h_lewis@126.com (H. Liu), 623340767@qq.com (H. Shi).
Peer review under responsibility of King Saud University.

Production and hosting by Elsevier

https://doi.org/10.1016/j.jsps.2019.08.002
1319-0164/

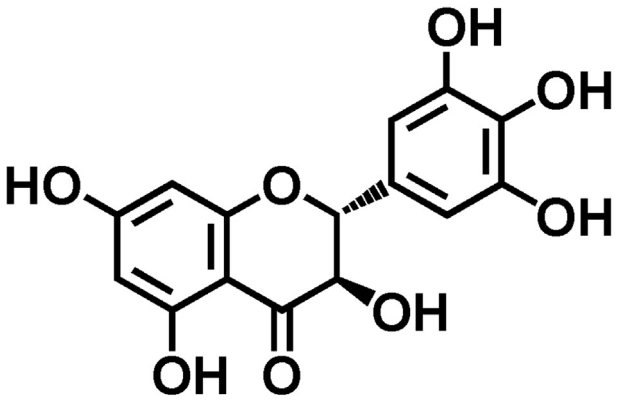

Fig. 1. The chemical structure of dihydromyricetin (DHM).

the drug or increase the apparent solubility of the drug. So far, several possible dosage forms based on drug carriers have been investigated in order to improve the solubility of DHM. These dosage forms include solid dispersion, inclusion complex, and microemulsion. The solid dispersion can inhibit the formation and growth of the drug crystal nucleus through the hydrogen bond and complexation between the carrier molecule and the drug. This ensures that the drug is highly dispersed in the carrier material with molecules or amorphous forms, which is conducive to the release of DHM, thus improving its solubility (Ruan et al., 2005; Suvarna et al., 2017). Inclusion complexes are compounds formed by complete or partial encapsulation of drug molecule in the cavity structure of the molecule of loading materials. Inclusion complexes are usually formed by Van der Waals force that can notably affect the rate of drug release. Microemulsion is a colloidal dispersion system with stable thermodynamic properties, which has the advantages of increasing the solubility of the drug and protecting the stability of drug from the external environment (Solanki et al., 2012). Despite these potential dosage forms, previous studies have mainly focused on the improvement of the water solubility of DHM, while the stability, pharmacokinetics, and bioavailability of the drug remain to be investigated. Additionally, the above dosage forms *per se* have shown shortcomings, such as non-controlled drug release and/or fast elimination. At the same time, due to the rapid metabolism of DHM and its short half-life *in vivo* (Liu et al., 2017; Huang et al., 2018), the previously reported preparations may require frequent administration in practices, thereby reducing the patient compliance.

Ideally, a suitable DHM preparation should be able to enhance or maintain the stability of the drug, meet the required doses, and promote the dispersion and dissolution of the drug in the aqueous phase. This is important in order to achieve higher bioavailability and better patient compliance. It should be noted that, since DHM is more stable in acidic conditions, release and absorption of this drug in the acidic environment of the stomach can probably be favorable, although the absorption site of DHM is not located only in stomach. During our previous investigation, it was found that the gastric floating sustained-release tablet could be a promising dosage form for DHM. Generally, the gastric floating sustained-release preparations consist of drugs, hydrophilic gel retention materials, foaming agents, and some other excipients (Gong et al., 2018). The gastric floating sustained-release system combines the advantages of both the gastric floating preparations and the sustained-release agents to realize the sustained release and absorption of the drug in the stomach. Sustained-release agents, particularly the sustained-release tablet as a widely used dosage form for oral administration, have the advantages of good drug loading capacity and sustained drug release for a long period of time (Anraku et al., 2019; Wang et al., 2019; Zhang et al., 2019). However, the retention time of conventional sustained-release agents in the gastrointestinal tract can be inadequate for full release of the drug, namely the drug may have left the absorption sites before it is fully released (Qi et al., 2015). In such case, the bioavailability of the drug may not be effectively improved. On the other hand, the gastric floating preparation is designed to have lower density than that of the stomach contents, so that it can float on the stomach contents for a long time. Compared with the conventional sustained-release preparation, the gastric floating sustained-release system is more resistant to the gastric emptying. This feature can not only prolong the time for the absorption and retention of the drug *in vivo*, but also help maintain the stability of DHM before absorption (Fu et al., 2018; Qin et al., 2018; Rahamathulla et al., 2019; Raza et al., 2019). Therefore, the gastric floating sustained-release tablet may improve the bioavailability of DHM through the sustained drug release in the stomach.

In this study, DHM-loaded gastric floating sustained-release tablets (DHM-GFTs) were prepared via a powder direct compression method (Fig. 2). The biocompatible polymer materials including polyvinylpyrrolidone (PVP), ethyl cellulose (EC), and

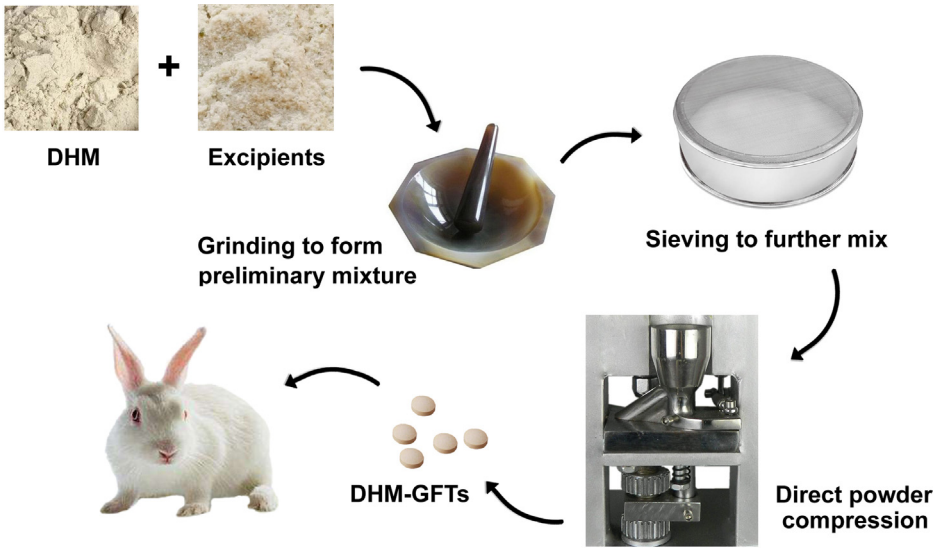

Fig. 2. Schematic representation for the preparation of DHM-GFTs.

Hydroxypropyl methyl cellulose (HPMC) were used to produce the tablets, and the formulation was optimized in terms of the floating ability and drug release rate. In addition, the physicochemical properties and *in vivo* pharmacokinetic behaviors of DHM-GFT were also studied.

2. Materials and methods

2.1. Materials

Dihydromyricetin (DHM, purity > 98%), lactose (anhydrous), ethyl cellulose (EC, viscosity 10 cP), magnesium stearate (Mg stearate), and sodium bicarbonate ($NaHCO_3$) were purchased from Shanghai Aladdin Bio-Chem Technology Co., Ltd., China. Dihydroquercetin (reference standard, purity > 98%) and PVP K30 were purchased from Sigma-Aldrich, Inc., USA. HPMC K4M was purchased from Ashland Inc., USA. The reagents above were used without further purification.

2.2. Preparation and optimization of DHM-GFTs

DHM-GFTs were prepared via the direct powder compression method which is a commonly used method for tablet manufacturing (Hamoudi-Ben Yelles et al., 2017; Karttunen et al., 2019; Nakamura et al., 2019). The schematic representation for the preparation process was shown in Fig. 2. First of all, 100 mg DHM, 100 mg HPMC, 50 mg lactose, 25 mg EC, 50–70 mg PVP, 45–75 mg $NaHCO_3$, and 3.7–4.2 mg Mg stearate were ground in a mortar to form a preliminary powder mixture, and were then passed through a 60-mesh screen for three times to thoroughly mix the drug and excipients. Afterwards, the uniform mixture was directly compressed into tablets weighing 200 mg on a ZP-12B single-punch tablet machine (Degong Machinery Equipment, China) equipped with an 8-mm flat-faced round punch. The force of compression was adjusted to obtain tablet hardness of 90 ± 5 N. The input amounts of PVP and $NaHCO_3$ were optimized according to the floating capacity and drug release rate of the tablets. The different formulations for DHM-GFT were as listed in Table 1.

2.3. Floating lag time and floating duration

The floating ability of DHM-GFTs was evaluated visually as described by Gong et al (2018). One tablet was put into a 1000-mL beaker filled with 900 mL HCl solution (pH 1.2). The medium was kept at 37 ± 0.5 °C, and was stirred at 100 rpm. The time that the tablet needed to rise onto the medium surface (i.e. the floating lag time), and the period during which the tablet kept buoyant (i.e. the floating duration) were recorded. The experiment of each formulation was done in triplicate.

2.4. In vitro drug release profile

The *in vitro* drug release of DHM-GFTs was investigated using the paddle method as described in previous literature (Gong et al., 2018). The experiments were done on a ZRS-12S dissolution apparatus (Tianjin Jingtuo Instrument Technology, China). Briefly, one tablet was put into the dissolution cup filled with 900 mL HCl solution (pH 1.2). The dissolution medium was kept at 37 ± 0.5 °C, and was stirred at 100 rpm. At predetermined time intervals, 1 mL medium was withdrawn and filtered using a 0.45 μm membrane. At the same time, 1 mL fresh medium was replenished. The amount of DHM released into the dissolution medium was then determined using high-performance liquid chromatography (HPLC). The sample (20 μL) was injected into a 1260 Infinity Ⅱ HPLC system (Agilent Technologies, USA) which was equipped with G7111B quaternary pump, G7129A automatic sampler, G7116A multicolumn thermostat, and G7114A variable wavelength detector. Separation was done at 25 °C on a reversed-phase C18 column (4.6 × 250 mm; Welch Materials, China) with particle size of 5 μm. The flow rate of mobile phase [acetonitrile-0.2% phosphoric acid solution (20:80, v/v)] was 1.0 mL/min. The samples were detected at 291 nm. The release experiments of tablets with different formulations were done in triplicate. The mechanism of drug release was studied using the Kopcha and Korsmeyer-Peppas models which are two commonly used models for understanding the release of drug (Kesarla et al., 2015; Acharya et al., 2014). The Kopcha equation is given as $Q_t/t = A/t^{1/2} + B$ (Asadian-Ardakani et al., 2016). The Korsmeyer-Peppas equation is given as $Q_t/Q_\infty = k_p t^n$. In these equations, t refers to the time; Q_t refers to the amount of drug released at time t; A and B are the relative contributions of diffusion and erosion, respectively; Q_t/Q_∞ is the fraction of drug release at time t; k_p is the release rate constant; and the n value indicates the mechanism of drug release (Asadian-Ardakani et al., 2016).

2.5. Characterization of optimized DHM-GFT

DHM-GFT with the optimal formulation (F6) was characterized in terms of the weight variation, drug content, thickness, diameter, hardness, and friability (Kaleemullah et al., 2017; Kesarla et al., 2015). To investigate the weight variation, twenty randomly selected DHM-GFTs were weighed individually (Kaleemullah et al., 2017). The weight of each tablet was then compared with the average weight of the twenty DHM-GFTs. For drug content, ten DHM-GFTs were weighed together and finely powdered. 50 mg of the powder was added into 100 mL 0.1 N HCl to extract the drug, which was followed by filtration using a 0.45 μm membrane (Kesarla et al., 2015). The drug content percentage of DHM-GFTs was then determined using HPLC as described above. For drug content uniformity, ten randomly selected tablets were tested individually. Each tablet was finely powdered and was added into 400 mL 0.1 N HCl to extract the drug, which was fol-

Table 1
Formulations of DHM-GFTs for optimization.

Formulation codes	DHM (mg)	HPMC (mg)	Lactose (mg)	EC (mg)	Mg stearate (mg)	PVP (mg)	$NaHCO_3$ (mg)	Theoretical drug content (%)
F1	100	100	50	25	3.70	50	45	26.76
F2	100	100	50	25	3.85	50	60	25.72
F3	100	100	50	25	4.00	50	75	24.75
F4	100	100	50	25	3.80	60	45	26.06
F5	100	100	50	25	3.95	60	60	25.07
F6	100	100	50	25	4.10	60	75	24.15
F7	100	100	50	25	3.90	70	45	25.39
F8	100	100	50	25	4.05	70	60	24.45
F9	100	100	50	25	4.20	70	75	23.57

lowed by filtration using a 0.45 μm membrane (Acharya et al., 2014). The drug content of each tablet was then determined using HPLC as described above. The thickness and diameter of DHM-GFTs were determined using a vernier caliper (Deli Group, China), for which ten randomly selected tablets were measured individually. The hardness and friability of DHM-GFTs were investigated using a ZPJ-6 tablet tester (Tianjin Jingtuo Instrument Technology, China). For hardness, ten randomly selected tablets were tested individually. For friability, thirty-three randomly selected DHM-GFTs (about 6.6 g in total) were weighed and put into the friability testing drum of the tablet tester. The drum was set to roll at 25 rpm for 4 min. Afterwards the tablets were de-dusted and weighed. The percent weight loss as the indicator for friability was calculated.

2.6. Studies on swelling and erosion

To study the swelling and erosion of optimized DHM-GFT, one tablet was weighed (w_0) and put into 900 mL 0.1 N HCl (pH 1.2) at 37 ± 0.5 °C. The medium was then stirred at 100 rpm. At predetermined time intervals, the tablet was gently taken out from the medium, and the liquid on its surface was removed using a filter paper. The tablet was then weighed (w_1), and dried at 50 °C in a DZF-6020 vacuum drying oven (Tianjin Gongxing Laboratory Instruments, China) until the tablet no longer changed in its weight (w_2). The degrees of swelling and erosion were evaluated as follows: swelling (%) = $(w_1 - w_0)/w_0 \times 100\%$; erosion (%) = $(w_0 - w_2)/w_0 \times 100\%$. The experiment on swelling and erosion was done in triplicate.

2.7. Animals

Albino New Zealand rabbits (2.0 ± 0.1 kg) were supplied by the Laboratory Animal Center of Southwest Medical University. The rabbits were kept under pathogen-free environment, with free access to food and water. The studies that involved animals have been approved by the Ethics Committee of Southwest Medical University (approval number: 201701200282).

2.8. Pharmacokinetic studies

The pharmacokinetic studies followed the methods as described by Huang et al (2016). The rabbits for pharmacokinetic study were fasted with free access to water for over 12 h before use. The rabbits (2.0 ± 0.1 kg) were randomly divided into three groups, each containing three male rabbits and three female rabbits, and were orally administered with five optimized DHM-GFTs (about 120.75 mg DHM/kg), ten optimized DHM-GFTs (about 241.50 mg DHM/kg), or 241.5 mg DHM powder (about 120.75 mg DHM/kg). At different time points after the administration, 1.2–1.5 mL blood samples were collected through the marginal ear vein of each animal. The blood samples were centrifuged at 5000 rpm for 10 min to obtain supernatant plasma. The concentration of DHM in the plasma sample was then determined using HPLC. For this purpose, 440 μL plasma was added with 60 μL methanol that contained 0.5 μg dihydroquercetin as the internal standard, and 500 μL acetate buffer (pH 4.5). After vortexed for 3 min, the mixture was added with 3 mL ethyl acetate, and was vortexed again for 5 min, followed by centrifugation at 5000 rpm for 10 min. Then 2.4 mL supernatant was withdrawn, and the organic solvent was evaporated via nitrogen flow. The dried residue was dissolved in 100 μL mobile phase, followed by centrifugation at 8000 rpm for 10 min. Afterwards the supernatant was analyzed using the HPLC system as described above. The maximum plasma concentration (C_{max}) of DHM and the time to reach C_{max} (t_{max}) were determined by observation (Gong et al., 2018). Other pharmacokinetic data were analyzed using the Drug and Statistics (DAS) 2.0 pharmacokinetics software (Chinese Pharmacological Society, China) which has been widely used for pharmacokinetic studies (Gong et al., 2018; Huang et al., 2016; Wang et al., 2018). Non-compartmental method based on the statistical moment theory that does not require the assumption of a specific compartment for drug was chosen for the calculations (Liu et al., 2015; Zhou et al., 2018; Song et al., 2015). The area under the plasma concentration-time curve (AUC) was calculated based on the trapezoidal rule (Song et al., 2015). The mean retention time (MRT) was taken as the time required for 63.2% of the drug to be eliminated from the body. The terminal elimination half-life ($t_{1/2(T-\infty)}$) was calculated as $0.693/k_{(T-\infty)}$, for which the $k_{(T-\infty)}$ referred to the terminal elimination rate constant. The relative bioavailability (F_R) of DHM-GFT as compared with DHM powder was calculated as follows (Wang et al., 2018): $F_R(\%) = (AUC_{0-\infty(\text{DHM-GFT})} \times \text{Dose}_{(\text{DHM powder})})/(AUC_{0-\infty(\text{DHM powder})} \times \text{Dose}_{(\text{DHM-GFT})}) \times 100\%$.

2.9. Statistical analysis

The differences of data were analyzed using Student's *t*-test for two groups and one-way ANOVA for multiple groups (Liu et al., 2019), using the Prism 5 (GraphPad, USA) as the analyzing software. $P < 0.05$ was considered statistically significant.

3. Results and discussion

3.1. Preparation of DHM-GFTs

Since DHM is more stable under acidic conditions, sustained release of DHM in the acidic environment in the stomach can not only prolong the time for the absorption and retention of the drug *in vivo*, but also help maintain the stability of DHM before absorption. Therefore, the DHM-GFT developed in this study may potentially improve the bioavailability of the drug and reduce the frequency of administration through the sustained release of DHM in the stomach. DHM-GFTs were obtained via direct compression of mixture powder consisting of DHM and different excipients. $NaHCO_3$ was used to generate carbon dioxide around DHM-GFT, which lowered the overall density of the tablets. Increasing the input amount of $NaHCO_3$ can result in an increased production rate of carbon dioxide in acidic environment and consequently shorter floating lag time (Gong et al., 2018). HPMC could form gel barriers around the tablet after hydration, which slowed down further hydration of the tablet and retained the carbon dioxide inside the gel for a longer floating duration (Acharya et al., 2014; Gong et al., 2018; Siepmann et al., 2017). Without the swollen gel, the carbon dioxide may leave the tablet more rapidly as the gastric contents move, leading to a relatively shorter floating duration. Moreover, the gel layer formed by HPMC could also lengthen the diffusion path of drug, realizing sustained release of DHM. During our pilot study, it was found that increasing the amount of HPMC could prolong both the floating lag time and the floating duration, and decrease the rate of drug release. For example, when the input amounts of the other components were the same as the formulation F5, increasing the amount of HPMC to 125 mg resulted in average floating lag time of about 41 s, average floating duration of about 20 h, and cumulative drug release at 20 h of <90%; while decreasing the amount of HPMC to 75 mg resulted in average floating lag time of about 10 s, average floating duration of about 11 h, and cumulative drug release at 8 h of over 90%. Therefore, too large amount of HPMC may lead to too long floating lag time and too slow drug release, while too small amount of HPMC may lead to too short floating duration and too fast drug release. Since HPMC alone has multiple effects on the tablets, its input amount has been

optimized in our previous study, in order to achieve suitable ranges of floating lag time, floating duration, and drug release rate for further optimization. PVP as a hydrophilic polymer could facilitate the erosion of tablets, which helps the dissolution of drug after hydration and results in a faster drug release (Park et al., 2015). EC as a hydrophobic polymer was used as the adhesive and hydrophobic matrix of DHM-GFT (Tolia and Li, 2014; Obiedallah et al., 2018). The introduction of EC could facilitate the formation of tablet and improve the resistance to shear forces. Lactose was used as the filler, which also helped the formation of tablet (Shojaee et al., 2016). The Mg stearate, required at low amount (about 1% of total tablet weight), worked as the lubricant for better preparation of tablets (Taipale-Kovalainen et al., 2018; Huang et al., 2019).

During our pilot studies, the materials for excipients and the input amounts of lactose, EC, and Mg stearate have been determined mainly according to the compressibility and flowability of the powder mixture, and the consequent formability of tablets (Gulsun et al., 2018; Tank et al., 2018). In addition, since the floating ability and sustained drug release are two important functions of DHM-GFT, and are greatly affected by the use of $NaHCO_3$ and PVP, the input amounts of the two components were optimized in the present study. The investigated formulations (F1-F9) for DHM-GFT were as listed in Table 1. Under the preparation conditions of this study, DHM-GFTs with the nine different formulations were all in good shapes with homogeneous appearances.

3.2. Floating ability of DHM-GFTs

The floating abilities of different DHM-GFTs were evaluated according to their floating lag time and floating duration (Kim et al., 2016; Thapa and Jeong, 2018). As shown in Fig. 3, the average floating lag time of DHM-GFT was within the range of 6.7–31.7 s, and the average floating duration was within the range of 8.8–17.0 h. Based on the floating durations, DHM-GFT can be developed as twice-a-day dosing preparation. As the input amount of PVP decreased or the input amount of $NaHCO_3$ increased, the floating lag time of DHM-GFT was shortened and the floating duration was prolonged. The carbon dioxide generated from $NaHCO_3$ could reduce the apparent density of the tablets, which enables the tablet to float (Acharya et al., 2014; Gong et al., 2018). It is no surprise to find that more $NaHCO_3$ resulted in shorter floating lag time and longer floating duration, since the amount of $NaHCO_3$ can affect the speed and amount of carbon dioxide production. More PVP resulted in shorter floating duration, because PVP is a hydrophilic polymer that can help the hydration and erosion of the tablet (Park et al., 2015). With faster hydration and erosion, the carbon dioxide produced from $NaHCO_3$ can detach from the tablet more rapidly, resulting in faster increase of the apparent density of tablet. However, the floating lag time was also notably affected by the amount of PVP, which was probably due to that larger amount of PVP has led to faster hydration of HPMC right after the tablet was put into the acid medium. With increased amount of PVP, HPMC in the tablet was hydrated more rapidly, and formed gel barriers that hindered the chemical reaction of $NaHCO_3$ with the gastric acid, resulting in slower production of carbon dioxide and consequently longer floating lag time. It is noteworthy that, both shorter floating lag time and longer floating duration are important for DHM-GFTs. On one hand, shorter floating lag time can help reduce the effects of gastric emptying on the tablets. On the other hand, longer floating duration can guarantee more sufficient time for sustained drug release. In this study, DHM-GFT F3 and F6 have respectively exhibited short floating lag time of <10 s on average, while DHM-GFT F1-F6 have respectively shown long floating duration of over 12 h on average. These results, combined with the results from drug release studies, were used for determination of the optimal formulation of DHM-GFT.

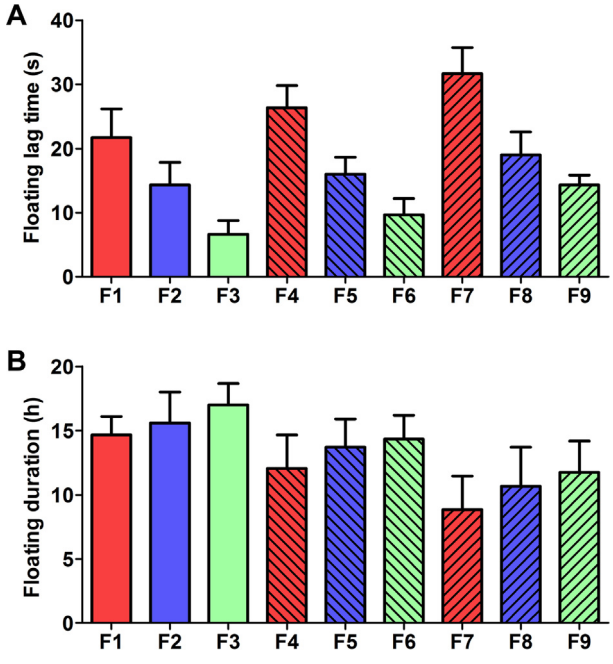

Fig. 3. The floating abilities of DHM-GFTs with different formulations (F1–F9) as evaluated according to their (A) floating lag time and (B) floating duration in the acidic medium. Data of each formulation were presented as mean ± SD (n = 3).

3.3. In vitro drug release profile of DHM-GFTs

The *in vitro* drug release profiles of DHM-GFTs with different formulations were shown in Fig. 4. All DHM-GFTs basically completed the release of DHM after 15 h. Nevertheless, within the first 15 h, the drug release of DHM-GFT was notably faster with increased amount of PVP. This was probably due to that, PVP could accelerate the hydration and erosion of the tablets, thus promoting the dissolution of the drug. Under the same conditions, the changes in the amount of $NaHCO_3$ showed very limited effects on the release rate of drug. It should be noted that, although sustained drug release is an essential requirement for DHM-GFT, completed drug release at expected time is also important for adequate drug efficacy and safety. Since the DHM-GFT was more likely to develop as a twice-a-day preparation, we focused on the degree of drug release at 12 h. At this time point, the average percentages of drug release were only about 85% for DHM-GFT with the lower amount of PVP (F1-F3), and were up to about 97% for DHM-GFT with the higher amount of PVP (F7-F9). Particularly, DHM-GFT F4-F9 showed the drug release of over 90% at 12 h, indicating almost completed drug release within half day.

In order to determine the optimal formulation of DHM-GFT, the results from the studies of both the drug release and the floating ability of DHM-GFTs were considered. The requirements that each formulation could satisfy were as summarized in Table 2. As a result, formulation F6 that satisfied all three requirements was determined as optimal for DHM-GFT, and was used both for characterization and for the subsequent studies. The floating lag time, floating duration, and 12 h cumulative drug release of DHM-GFT F6 were 9.67 ± 2.52 s, 14.33 ± 1.86 h, and 94.06% ± 1.47%, respectively.

3.4. Characterization of DHM-GFT with the optimal formulation (F6)

The weight of the optimized DHM-GFT, as investigated using twenty randomly selected tablets, was 199.87 ± 1.15 mg (Table 3).

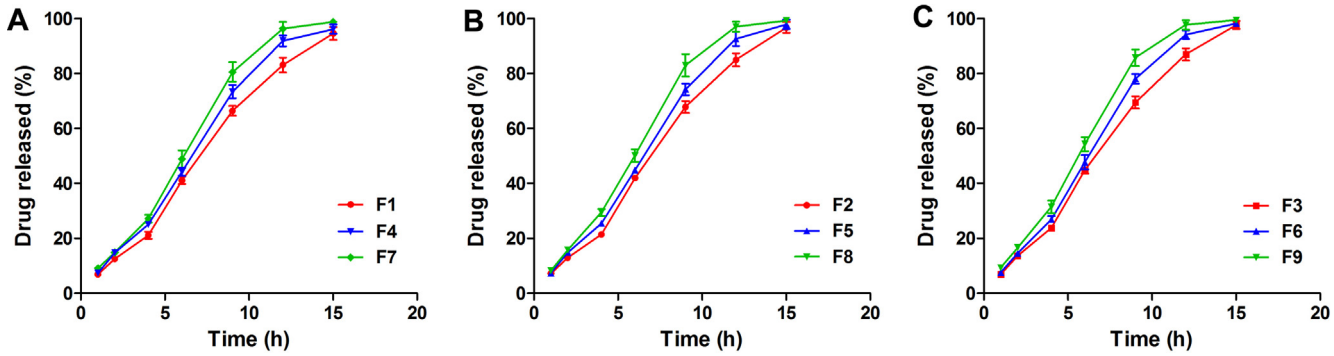

Fig. 4. The *in vitro* drug release profiles of DHM-GFTs with the formulations (A) F1, F4, F7 with lower amount of $NaHCO_3$; (B) F2, F5, F8 with medium amount of $NaHCO_3$; and (C) F3, F6, F9 with higher amount of $NaHCO_3$. Data of different time points of each formulation were presented as mean ± SD (n = 3).

Table 2
List of the requirements satisfied by each formulation.

Requirements[a]	F1	F2	F3	F4	F5	F6	F7	F8	F9
Floating lag time < 10 s			√			√			
Floating duration > 12 h	√	√	√	√	√	√			
Cumulative drug releasewithin 12 h > 90%				√	√	√	√	√	√

[a] The tick ("√") indicates that the formulation meets the corresponding requirement. Formulation F6 met all three requirements, and was therefore determined as optimal for DHM-GFT.

Table 3
The characterization results of DHM-GFT with the optimal formulation (F6).

Evaluation items for tablet	Measured values[a]	Theoretical values or pharmacopoeial requirements
Weight (mg)	199.87 ± 1.15	200
Drug content percentage (%)	24.02 ± 0.32	24.15
Drug content per tablet (mg)	48.23 ± 0.25	48.30
Thickness (mm)	3.66 ± 0.04	Not specified
Diameter (mm)	8.01 ± 0.03	8
Hardness (N)	88.2 ± 2.9	90 ± 5
Friability (%)	0.51 ± 0.06	<1

[a] Data are presented as mean ± SD.

The difference between the measured weight of DHM-GFT and the expected weight (i.e. 200 mg) was within 1%. Moreover, the difference between the weight of each tablet and the average weight of the twenty tablets (i.e. 199.87 mg) was within 1.5%. The drug content percentage, thickness, and diameter of DHM-GFT were 24.02% ± 0.32%, 3.66 ± 0.04 mm, and 8.01 ± 0.03 mm, respectively. The drug content per tablet was 48.23 ± 0.25 mg. The differences between these measured values and the theoretical values were within 1%, which indicated good uniformity of the tablets. It is noteworthy that, the drug content is not necessarily affected by the weight of the tablet, because the drug content reflects the weight percentage of the drug in the tablet, while the weight of the tablet reflects the total weight of the drug and the excipients in the tablet. The hardness of DHM-GFT was 88.2 ± 2.9 N, which was within the expected range of 90 ± 5 N. It should also be noted that, the hardness can notably affect the mechanical strength and density of the tablet (Gulsun et al., 2018; May et al., 2013). It was found during our pilot investigation that, the hardness of about 90 N was suitable to achieve both adequate mechanical strength and proper densities for DHM-GFT. When the hardness was too low (e.g. <80 N), the tablets disintegrated rapidly in the dissolution medium. When the hardness increased, both the mechanical strength and density of tablets increased. With the hardness of about 90 N, the density of DHM-GFT was near 1 g/cm^3 (close to the density of the dissolution medium), which was favorable to achieve good floating ability of the tablet. However, when the hardness was too high (e.g. >100 N), it was noticed that the density of DHM-GFT became too large, and the tablets could hardly float even when a large amount of $NaHCO_3$ was added. Therefore, the tablet hardness of 90 ± 5 N was considered to be suitable for DHM-GFT. The friability of DHM-GFT was 0.51% ± 0.06%, which was within 1%. It is a pharmacopoeial requirement that, for fragility study of tablet that weighs <0.65 g, tablets with a total weight of about 6.5 g should be used for each experiment (Chinese Pharmacopoeia Commission, 2015). Therefore, this study used thirty-three tablets with a total weight of about 6.6 g in each experiment of fragility study to meet the requirement as precisely as possible. The results above well met the requirements of Chinese Pharmacopoeia for tablets (Table 3), demonstrating the good quality of DHM-GFT.

3.5. Swelling and erosion of DHM-GFT

The swelling and erosion profiles of the optimized DHM-GFT, as investigated via gravimetric measurement at different time points, were presented in Fig. 5. The drug release profile of DHM-GFT was also presented for the analysis (Fig. 5A). According to Fig. 5B, the tablets exhibited fast swelling rate in the first 6 h. However, the percentage of swelling started to decrease dramatically after 6 h due to increasingly larger degree of erosion (Fig. 5C). Additionally, the data of drug release were fitted using the Kopcha and Korsmeyer-Peppas equations for understanding the release of drug. The fitted equation for the drug release of the optimized DHM-GFT was $Q_t/t = 0.295/t^{1/2} + 3.516$ ($R^2 = 0.921$) using the Kopcha model, and was $Q_t/Q_\infty = 0.075\ t^{0.998}$ ($R^2 = 0.990$) using the Korsmeyer-Peppas model. According to the Korsmeyer-Peppas equation, the n value was 0.998, which indicated a non-Fickian release or anomalous transport and that the drug release was regulated by both diffusion and erosion (Acharya et al., 2014). Furthermore, the fitting results from the Kopcha model could to some extent indicate the relative contributions of diffusion (the A value) and erosion (the B value) to the drug release (Asadian-Ardakani et al, 2016). It could be seen that B (i.e. 3.516) is much greater than

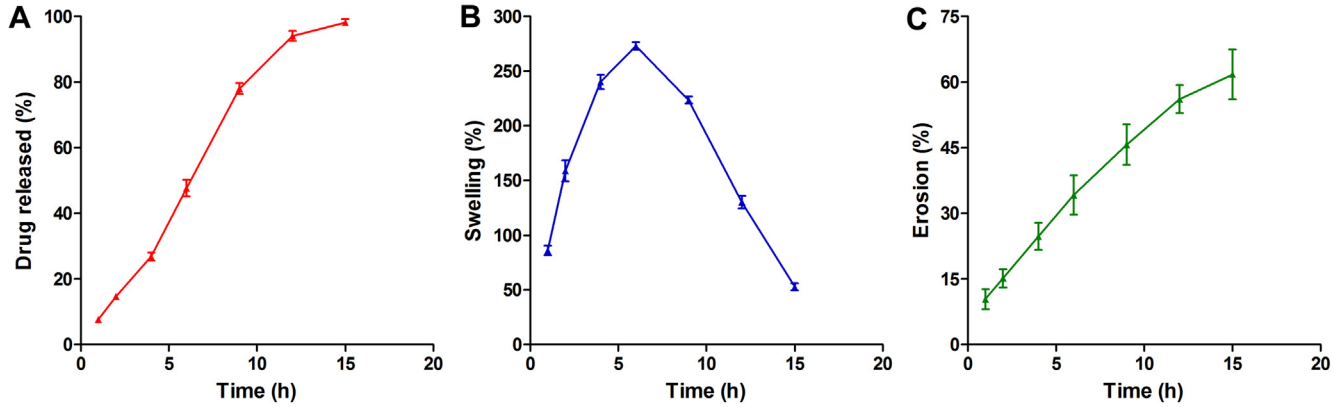

Fig. 5. (A) Drug release, (B) swelling, and (C) erosion profiles of the optimized DHM-GFT (formulation F6) in the acidic medium. Data of different time points were presented as mean ± SD (n = 3).

A (i.e. 0.295), indicating that the drug release from DHM-GFT was mainly controlled by the erosion.

Based on the results above, some important changes in the tablet after its introduction to the dissolution medium can be speculated. At the beginning, the medium penetrated into the tablet, and the tablet started to swell and undergo erosion. During this process, the $NaHCO_3$ reacted with the acid in the medium to produce carbon dioxide, and the tablet started to rise onto the medium surface. At the same time, HPMC close to the tablet surface was hydrated, and produced a gel layer around the tablet which preserved the carbon dioxide but also slowed down the dissolution of DHM. This resulted in relatively smaller slope of the drug release profile for the first 4 h (Fig. 5A). However, as the percentage of swelling and erosion went on increasing, the gel layer started to dissolve. With the help of PVP (the water absorbent), more and more drug was released from the tablet, leading to fast release rate after 4 h. At 8 h, the erosion of tablet was around 45% (Fig. 5C). At the same time point, most of DHM (near 80%) has been released from the tablet, and the release rate started to decrease (Fig. 5A).

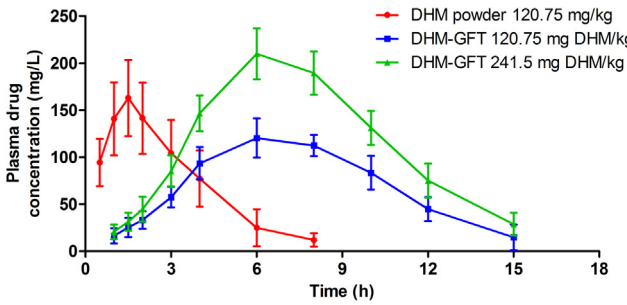

Fig. 6. The plasma concentration-time curves of DHM powder and DHM-GFT at different doses. Data of different time points of each group were presented as mean ± SD (n = 6). Compared to DHM powder, DHM-GFT showed much prolonged drug residence time.

3.6. Pharmacokinetic studies

In order to study the pharmacokinetic behaviors of the optimized DHM-GFT, rabbits were orally administered with DHM-GFT at 120.75 or 241.50 mg DHM/kg, or DHM powder at 120.75 mg/kg as the control. The plasma concentration-time curves of different groups were presented in Fig. 6. The pharmacokinetic parameters as determined by non-compartmental analyses were summarized in Table 4. For DHM powder group, the C_{max} appeared at 1.5 h after the administration, and was 163.11 ± 40.49 μg/L. By contrast, DHM-GFT at the same dose level had significantly longer ($P < 0.001$) t_{max} of 6.67 ± 1.03 h, which was probably due to the sustained release of DHM from DHM-GFT. On one hand, the release process of DHM-GFT could to some extent slow down the absorption of DHM, resulting in relatively slower increase of the plasma drug concentration and consequently prolonged t_{max}. On the other hand, the absorbed drug was being cleared from the plasma. Since t_{max} of DHM-GFT group 1 was significantly longer as compared to DHM powder group, a larger amount of absorbed drug may have been cleared from the plasma during this period of time, which resulted in a lower C_{max} (Huang et al., 2016; Qin et al., 2018). Besides, DHM-GFT group 1 exhibited longer $MRT_{0\text{-}T}$ (6.78 ± 0.17 h vs. 2.42 ± 0.16 h, $P < 0.001$), $MRT_{0\text{-}\infty}$

Table 4
Pharmacokinetic parameters of DHM-GFTs and DHM powder in rabbits at different dose levels.

Pharmacokinetic parameters[a]	DHM powder at 120.75 mg/kg (DHM powder group)	DHM-GFT at 120.75 mg/kg (DHM-GFT group 1)	DHM-GFT at 241.5 mg/kg (DHM-GFT group 2)
t_{max} (h)	1.50 ± 0.00	6.67 ± 1.03***	6.00 ± 0.00
C_{max} (μg/L)	163.11 ± 40.49	123.35 ± 16.17	210.05 ± 27.28
$AUC_{0\text{-}T}$ (μg·h/L)	550.31 ± 173.77	925.22 ± 147.53**	1662.20 ± 231.99
$AUC_{0\text{-}\infty}$ (μg·h/L)	605.20 ± 224.68	1076.24 ± 181.23**	1757.03 ± 272.03
$MRT_{0\text{-}T}$ (h)	2.42 ± 0.16	6.78 ± 0.17***	7.40 ± 0.23
$MRT_{0\text{-}\infty}$ (h)	2.85 ± 0.57	7.97 ± 0.64***	7.97 ± 0.48
$t_{1/2(T\text{-}\infty)}$ (h)	1.17 ± 0.58	2.26 ± 0.49**	2.14 ± 0.46
F_R (%)		177.83	145.16

**P < 0.01 and ***P < 0.001, as compared with DHM powder at the same dose level.

[a] Data are presented as mean ± SD, n = 6. C_{max}: maximum plasma concentration. t_{max}: time needed to reach C_{max}. $AUC_{0\text{-}T}$: area under the plasma concentration-time curve for 0 h to the last time point of measurement. $AUC_{0\text{-}\infty}$: area under the whole plasma concentration-time curve. $MRT_{0\text{-}T}$: mean retention time for 0 h to the last time point of measurement. $MRT_{0\text{-}\infty}$: mean retention time for the whole plasma concentration-time curve. $t_{1/2(T\text{-}\infty)}$: terminal elimination half-life, namely the half life for the period after the last time point of measurement. F_R: relative bioavailability.

(7.97 ± 0.64 h vs. 2.85 ± 0.57 h, $P < 0.001$), and $t_{1/2(T-\infty)}$ (2.26 ± 0.49 h vs. 1.17 ± 0.58 h, $P < 0.01$) as compared with DHM powder group. These results suggested slower absorption and elimination of drug, which was mainly due to the sustained drug release of the tablets. The AUC_{0-T} and $AUC_{0-\infty}$ of DHM-GFT group 1 were 925.22 ± 147.53 μg·h/L and 1076.24 ± 181.23 μg·h/L, respectively, which were also significantly larger than those of the DHM powder group ($P < 0.01$). Moreover, the F_R of DHM-GFT group 1 was 177.83%, far beyond 100%. DHM powder group exhibited much smaller AUCs, which was probably due to that most of the drug powder has left stomach before absorbed, and in the alkaline environment of intestine the drug molecules degenerated, leading to poor bioavailability. The results above demonstrated that, DHM-GFT has maintained the stability and prolonged the residence time of DHM via its good gastric floating ability and sustained drug release, resulting in significantly improved bioavailability of the drug.

It is also noteworthy that, the t_{max}, MRT_{0-T}, $MRT_{0-\infty}$, and $t_{1/2(T-\infty)}$ of DHM-GFT at an increased dose level (DHM-GFT group 2) were 1.50 ± 0.00 h, 2.42 ± 0.16 h, 2.85 ± 0.57 h, and 1.17 ± 0.58 h, respectively, which were similar with those of DHM-GFT group 1 (Table 4). Generally, the plasma concentration–time curves of DHM-GFT group 1 and group 2 exhibited similar shape, with evidently less sharp peak at t_{max} as compared to that of the DHM powder group (Fig. 6). This result indicated that, DHM-GFT has the potential to help maintain more steady plasma drug concentration as compared to DHM powder.

4. Conclusions

In this study, gastric floating sustained-release tablets for DHM (DHM-GFTs) were successfully prepared using the powder direct compression method, and the tablet formulation was optimized. DHM-GFT with the optimal formulation exhibited short floating lag time of <10 s and long floating duration of over 12 h in acidic medium (i.e. pH 1.2 HCl solution). It had a sustained release of DHM for about 12 h, which indicated the potential of DHM-GFT to be developed as a twice-a-day dosing preparation. The optimized DHM-GFT had the weight variation of <1.5% and the friability of <1%, which well satisfied the pharmacopoeial requirements. DHM-GFT went through notable swelling and erosion in the acidic medium, and the fitting results using kinetics models indicated that the drug release from DHM-GFT may be regulated by both the diffusion of the drug and erosion of the tablet matrix. In addition, the pharmacokinetic studies showed that the orally administered DHM-GFT at the dose of 120.75 mg DHM/kg had the MRTs of around 7 h and the AUCs of around 1000 μg·h/L in rabbits, which were significantly larger than those of the DHM powder group. These results demonstrated that, compared to DHM powder, DHM-GFT could considerably prolong the residence time of drug *in vivo* and improve the bioavailability via its good gastric floating ability and sustained drug release in the acidic environment. Therefore, DHM-GFT is a promising preparation for DHM, with the great potential to promote the clinical applications of this natural drug. Nevertheless, a more systematic investigation on how GFT affects the stability, release, bioavailability, and efficacy of the drug should be conducted in the near future for further development of this preparation.

Acknowledgements

This study was financially supported by Sichuan Science and Technology Program Project (2019YJ0489), the Research Project of Health and Family Planning Commission of Sichuan Province (16PJ536), Doctoral Research Start-up Fund of Southwest Medical University (to Hao Liu), the Research Project of National Undergraduate Innovation and Entrepreneurship Training Program (201810632064), and the Research Project of Undergraduate Innovation and Entrepreneurship Training Program of Southwest Medical University (2019448 and 2019501). The authors thank Southwest Medical University and the Affiliated Traditional Chinese Medicine Hospital of Southwest Medical University for their management.

Declaration of Competing Interest

None.

References

Acharya, S., Patra, S., Pani, N.R., 2014. Optimization of HPMC and carbopol concentrations in non-effervescent floating tablet through factorial design. Carbohyd. Polym. 102, 360–368. https://doi.org/10.1016/j.carbpol.2013.11.060.

Anraku, M., Tabuchi, R., Goto, M., Iohara, D., Mizukai, Y., Maezaki, Y., Michihara, A., Kadowaki, D., Otagiri, M., Hirayama, F., 2019. Design and evaluation of an extended-release olmesartan tablet using chitosan/cyclodextrin composites. Pharmaceutics 11 (2), 82. https://doi.org/10.3390/pharmaceutics11020082.

Asadian-Ardakani, V., Saber-Samandari, S., Saber-Samandari, S., 2016. The effect of hydroxyapatite in biopolymer-based scaffolds on release of naproxen sodium. J. Biomed. Mater. Res. A. 104 (12), 2992–3003. https://doi.org/10.1002/jbm.a.35838.

Chinese Pharmacopoeia Commission, 2015. Pharmacopoeia of the People's Republic of China. China Medical Science Press, Beijing.

Fu, J., Yin, H., Yu, X., Xie, C., Jiang, H., Jin, Y., Sheng, F., 2018. Combination of 3D printing technologies and compressed tablets for preparation of riboflavin floating tablet-in-device (TiD) systems. Int. J. Pharmaceut. 549 (1–2), 370–379. https://doi.org/10.1016/j.ijpharm.2018.08.011.

Gong, L., Sun, Y., Yu, M., Gao, Y., Zou, M., Cheng, G., 2018. Development and evaluation of compression coating gastro-floating tablet of alfuzosin hydrochloride for zero-order controlled release. AAPS Pharmscitech. 19 (7), 3277–3286. https://doi.org/10.1208/s12249-018-1168-z.

Gulsun, T., Akdag Cayli, Y., Izat, N., Cetin, M., Oner, L., Sahin, S., 2018. Development and evaluation of terbutaline sulfate orally disintegrating tablets by direct compression and freeze drying methods. J. Drug Deliv. Sci. Tec. 46, 251–258. https://doi.org/10.1016/j.jddst.2018.05.014.

Hamoudi-Ben Yelles, M.C., Tran Tan, V., Danede, F., Willart, J.F., Siepmann, J., 2017. PLGA implants: how poloxamer/PEO addition slows down or accelerates polymer degradation and drug release. J. Control. Release 253, 19–29. https://doi.org/10.1016/j.jconrel.2017.03.009.

Huang, C., Klinzing, G., Procopio, A., Yang, F., Ren, J., Burlage, R., Zhu, L., Su, Y., 2019. Understanding compression-induced amorphization of crystalline posaconazole. Mol. Pharmaceut. 16 (2), 825–833. https://doi.org/10.1021/acs.molpharmaceut.8b01122.

Huang, Y., Wei, Y., Yang, H., Pi, C., Liu, H., Ye, Y., Zhao, L., 2016. A 5-fluorouracil-loaded floating gastroretentive hollow microsphere: development, pharmacokinetic in rabbits, and biodistribution in tumor-bearing mice. Drug Des. Dev. Ther. 10, 997–1008. https://doi.org/10.2147/DDDT.S97735.

Huang, Y., Zhao, J., Jian, W., Wang, G., 2018. Effects of verapamil on the pharmacokinetics of dihydromyricetin in rats and its potential mechanism. Xenobiotica 48 (8), 839–844. https://doi.org/10.1080/00498254.2017.1366576.

Kaleemullah, M., Jiyauddin, K., Thiban, E., Rasha, S., Al-Dhalli, S., Budiasih, S., Gamal, O.E., Fadli, A., Eddy, Y., 2017. Development and evaluation of Ketoprofen sustained release matrix tablet using Hibiscus rosa-sinensis leaves mucilage. Saudi Pharm. J. 25 (5), 770–779. https://doi.org/10.1016/j.jsps.2016.10.006.

Karttunen, A.P., Wikstrom, H., Tajarobi, P., Fransson, M., Sparen, A., Marucci, M., Ketolainen, J., Folestad, S., Korhonen, O., Abrahmsen-Alami, S., 2019. Comparison between integrated continuous direct compression line and batch processing - the effect of raw material properties. Eur. J. Pharm. Sci. 133, 40–53. https://doi.org/10.1016/j.ejps.2019.03.001.

Kesarla, R.S., Vora, P.A., Sridhar, B.K., Patel, G., Omri, A., 2015. Formulation and evaluation of floating tablet of H2-receptor antagonist. Drug Dev. Ind. Pharm. 41 (9), 1499–1511. https://doi.org/10.3109/03639045.2014.959969.

Kim, J.S., Cha, K.H., Kang, S.Y., Won, D., Jang, S.W., Son, M., Son, M.H., Choi, H.J., Lee, Y.W., Kang, M.J., 2016. In vivo gastric residence and gastroprotective effect of floating gastroretentive tablet of DA-9601, an extract of Artemisia asiatica, in beagle dogs. Drug Des. Dev. Ther. 10, 1917–1925. https://doi.org/10.2147/DDDT.S102918.

Li, H., Yu, F., Sun, X., Xu, L., Miu, J., Xiao, P., 2019. Dihydromyricetin ameliorates memory impairment induced by acute sleep deprivation. Eur. J. Pharmacol. 853, 220–228. https://doi.org/10.1016/j.ejphar.2019.03.014.

Li, T., Yan, F., Meng, X., Wang, J., Ting Kam, R.K., Zeng, X., Liu, Z., Zhou, H., Yang, F., Ren, R., et al., 2018. Improvement of glucocorticoid-impaired thymus function by dihydromyricetin via up-regulation of PPARgamma-associated fatty acid metabolism. Pharmacol. Res. 137, 76–88. https://doi.org/10.1016/j.phrs.2018.09.011.

Liu, C., Wang, S.J., Zhang, Q., Shao, Y.X., 2015. Influence of three coccidiostats on the pharmacokinetics of florfenicol in rabbits. Exp. Anim. 64 (1), 73–79. https://doi.org/10.1538/expanim.14-0064.

Liu, H., Zhou, X., Wang, Y., Yang, M., Xu, X., Wu, A., 2019. Mixed micelle as nanocarrier for etomidate: Development, in vitro characterizations, and in vivo study on toxicity and anesthetic effects. J. Drug Deliv. Sci. Tec. 49, 123–131. https://doi.org/10.1016/j.jddst.2018.10.038.

Liu, L., Yin, X., Wang, X., Li, X., 2017. Determination of dihydromyricetin in rat plasma by LC-MS/MS and its application to a pharmacokinetic study. Pharm. Biol. 55 (1), 657–662. https://doi.org/10.1080/13880209.2016.1266669.

May, R.K., Su, K., Han, L., Zhong, S., Elliott, J.A., Gladden, L.F., Evans, M., Shen, Y., Zeitler, J.A., 2013. Hardness and density distributions of pharmaceutical tablets measured by terahertz pulsed imaging. J. Pharm. Sci. 102 (7), 2179–2186. https://doi.org/10.1002/jps.23560.

Nakamura, S., Tanaka, C., Yuasa, H., Sakamoto, T., 2019. Utility of microcrystalline cellulose for improving drug content uniformity in tablet manufacturing using direct powder compression. AAPS Pharmscitech. 20 (4), 151. https://doi.org/10.1208/s12249-019-1365-4.

Obiedallah, M.M., Abdel-Mageed, A.M., Elfaham, T.H., 2018. Ocular administration of acetazolamide microsponges in situ gel formulations. Saudi Pharm. J. 26 (7), 909–920. https://doi.org/10.1016/j.jsps.2018.01.005.

Park, J.B., Park, Y.J., Kang, C.Y., Lee, B.J., 2015. Modulation of microenvironmental pH and utilization of alkalizers in crystalline solid dispersion for enhanced solubility and stability of clarithromicin. Arch. Pharm. Res. 38 (5), 839–848. https://doi.org/10.1007/s12272-014-0471-9.

Qi, X., Jiang, Y., Zhang, H., Wu, Z., 2015. Tablets compressed with gastric floating pellets coated with acrylic resin for gastro retention and sustained release of famotidine: in-vitro and in-vivo study. J. Pharm. Pharmacol. 67 (4), 493–500. https://doi.org/10.1111/jphp.12339.

Qin, C., Wu, M., Xu, S., Wang, X., Shi, W., Dong, Y., Yang, L., He, W., Han, X., Yin, L., 2018. Design and optimization of gastro-floating sustained-release tablet of pregabalin: In vitro and in vivo evaluation. Int. J. Pharmaceut. 545 (1–2), 37–44. https://doi.org/10.1016/j.ijpharm.2018.04.011.

Rahamathulla, M., Saisivam, S., Gangadharappa, H.V., 2019. Development of Valsartan floating matrix tablets using low density polypropylene foam powder: in vitro and in vivo evaluation. AAPS Pharmscitech. 20 (1), 35. https://doi.org/10.1208/s12249-018-1265-z.

Raza, A., Shen, N., Li, J., Chen, Y., Wang, J.Y., 2019. Formulation of zein based compression coated floating tablets for enhanced gastric retention and tunable drug release. Eur. J. Pharm. Sci. 132, 163–173. https://doi.org/10.1016/j.ejps.2019.01.025.

Ruan, L.P., Yu, B.Y., Fu, G.M., Zhu, D.N., 2005. Improving the solubility of ampelopsin by solid dispersions and inclusion complexes. J. Pharmaceut. Biomed. 38 (3), 457–464. https://doi.org/10.1016/j.jpba.2005.01.030.

Shojaee, S., Kaialy, W., Cumming, K.I., Nokhodchi, A., 2016. Comparative evaluation of drug release from aged prolonged polyethylene oxide tablet matrices: effect of excipient and drug type. Pharm. Dev. Technol. 21 (2), 189–195. https://doi.org/10.3109/10837450.2014.982823.

Siepmann, F., Karrout, Y., Gehrke, M., Penz, F.K., Siepmann, J., 2017. Limited drug solubility can be decisive even for freely soluble drugs in highly swollen matrix tablets. Int. J. Pharmaceut. 526 (1–2), 280–290. https://doi.org/10.1016/j.ijpharm.2017.05.001.

Solanki, S.S., Sarkar, B., Dhanwani, R.K., 2012. Microemulsion drug delivery system: for bioavailability enhancement of ampelopsin. ISRN pharm. 2012, 108164. https://doi.org/10.5402/2012/108164.

Song, S., Chen, F., Xing, X., Ren, M., Ma, Q., Xie, Y., Tang, Q., Luo, J., 2015. Concurrent quantification and comparative pharmacokinetic analysis of bioactive compounds in the Herba Ephedrae-Semen Armeniacae Amarum herb pair. J. Pharmaceut. Biomed. 109, 67–73. https://doi.org/10.1016/j.jpba.2015.02.004.

Suvarna, V., Gujar, P., Murahari, M., 2017. Complexation of phytochemicals with cyclodextrin derivatives – an insight. Biomed. Pharmacother. 88, 1122–1144. https://doi.org/10.1016/j.biopha.2017.01.157.

Taipale-Kovalainen, K., Karttunen, A.P., Ketolainen, J., Korhonen, O., 2018. Lubricant based determination of design space for continuously manufactured high dose paracetamol tablets. Eur. J. Pharm. Sci. 115, 1–10. https://doi.org/10.1016/j.ejps.2017.12.021.

Tank, D., Karan, K., Gajera, B.Y., Dave, R.H., 2018. Investigate the effect of solvents on wet granulation of microcrystalline cellulose using hydroxypropyl methylcellulose as a binder and evaluation of rheological and thermal characteristics of granules. Saudi Pharm. J. 26 (4), 593–602. https://doi.org/10.1016/j.jsps.2018.02.007.

Thapa, P., Jeong, S.H., 2018. Effects of formulation and process variables on gastroretentive floating tablets with a high-dose soluble drug and experimental design approach. Pharmaceutics 10 (3). https://doi.org/10.3390/pharmaceutics10030161.

Tolia, G., Li, S.K., 2014. Silicone adhesive matrix of verapamil hydrochloride to provide pH-independent sustained release. AAPS Pharmscitech. 15 (1), 1–10. https://doi.org/10.1208/s12249-013-0004-8.

Wang, S., Wen, H., Li, P., Cui, M., Sun, W., Wang, H., Liu, H., Li, S., Pan, W., Yang, X., 2019. Formulation and evaluation of gastric-floating controlled release tablets of Ginkgolides. J. Drug Deliv. Sci. Tec. 51, 7–17. https://doi.org/10.1016/j.jddst.2019.02.011.

Wang, Y., Wang, Y., Wang, J., Lei, W., Li, K., Wu, D., Wang, X., 2018. Pharmacokinetics, biodistribution, and bioavailability of gossypol-loaded Pluronic® F127 nanoparticles. J. Drug Deliv. Sci. Tec. 45, 388–396. https://doi.org/10.1016/j.jddst.2018.04.002.

Xiang, D., Fan, L., Hou, X.L., Xiong, W., Shi, C.Y., Wang, W.Q., Fang, J.G., 2018. Uptake and transport mechanism of dihydromyricetin across human intestinal Caco-2 cells. J. Food Sci. 83 (7), 1941–1947. https://doi.org/10.1111/1750-3841.14112.

Zhang, J., Chen, Y., Luo, H., Sun, L., Xu, M., Yu, J., Zhou, Q., Meng, G., Yang, S., 2018. Recent update on the pharmacological effects and mechanisms of dihydromyricetin. Front. Pharmacol. 9, 1204. https://doi.org/10.3389/fphar.2018.01204.

Zhang, Y., Xu, B., Wang, X., Dai, S., Shi, X., Qiao, Y., 2019. Optimal selection of incoming materials from the inventory for achieving the target drug release profile of high drug load sustained-release matrix tablet. AAPS Pharmscitech. 20 (2), 76. https://doi.org/10.1208/s12249-018-1268-9.

Zhou, J., Li, M., Jin, W., Li, X., Fan, H., Zhang, Y., 2018. Pharmacokinetic study on protocatechuic aldehyde and hydroxysafflor yellow A of danhong injection in rats with hyperlipidemia. Pharmacology 102 (3–4), 154–160. https://doi.org/10.1159/000491020.